Journal of Applied Science and Engineering, Vol. 22, No. 4, pp. 699–707 (2019) DOI: 10.6180/jase.201912_22(4).0012

Generation of Multifractal Radioelectric Spectrum Traffic

Cesar Hernandez[1]* and Luis Tuberquia-David[2]

[1]Universidad Distrital Francisco José de Caldas, Technological Faculty, Calle 68D Bis A Sur # 49F - 70 Bloque 6, piso 1. Bogotá, Colombia
[2]Universidad Distrital Francisco José de Caldas, Faculty of Engineering, Carrera 7 # 40B–53. Bogotá, Colombia

Abstract

The growing use of communication networks in radio electric spectrum applications has reached a saturation point. Spectral prediction has gained importance, as several models have been studied to improve the accuracy of predicted traffic compared to real traffic. This research aims to generate a spectrum prediction method within a radio electric space. The obtained traffic is generated with the MFHW algorithm, which creates traces based on parameters given by the user: mean, Hurst parameter and spectrum width. The results revealed marginal errors of 0.04% for the Hurst parameter and 0.085% for the estimation of the multifractal spectrum width. The MFHW algorithm builds traces with self-similarity, long-range dependence (LRD), and multifractal characteristics, inherent to the behavior of the radioelectric spectrum. Hence, the method discussed in this paper can establish a modeling framework for the generation of traces applied to spectrum prediction based on multifractal analysis.

Key Words: Traffic Generation, Multifractal, Spectrum, Wireless Communication

1. Introduction

Future wireless communication systems are designed to support a wide range of services, such as multimedia traffic, streaming calls, cloud-based buffer upload and download. The use and demand of wireless data have recently risen, which is a trend expected to continue in wireless applications. It is likely that the monthly use of mobile data will increase by eight times before 2020 compared to 2015 [1]. The growing proliferation of wireless devices has congested the 900 MHz and 2.4 GHz bands. Meanwhile, several frequency bands licensed for operators in the 400–700 MHz range are used sporadically [2]. This notorious demand requires tools that can reduce congestion in current telecommunication networks.

One alternative to achieve this is spectrum prediction trying to straighten the use of communication channels. It is a promising approach that enhances cognitive radio functions. Extensive research has been carried out on various prediction techniques and applications in telecommunication networks. However, it still needs further effort in developing spectrum prediction designs, providing accurate long-range predictions, and defining prediction schemes for licensed users [3]. Over the years, spectral inference has shaped the occupation and characteristics of primary user activity. However, in the active detection process, there is a difficult circulation and control in current networks [4]. To overcome these issues, prediction strategies have been presented and widely studied.

Frisch et al. introduced the multiplicative cascade model in the context of turbulence analysis in the late 1980s [5]. Since the work of Leland et al. [6], several studies have shown that network traffic is scale-invariant, meaning that there is no specific timescale to characterize the burstiness of the traffic stream. Relevant stud-

*Corresponding author. E-mail: cahernandezs@udistrital.edu.co

ies have evidenced scale invariance such as the self-similar traffic model based on the ON-OFF model proposed by Taqqu et al. [7] and the multifractal formalism described by Riedi et al. in [8]. The latter has received wide attention as one of the most popular frameworks used to describe and analyze signals and processes with scaling properties, covering and connecting both local and global scaling regarding sample moments. Last but not least, Ma and Ji proposed Wavelet-based models [9]. All of the mentioned methods describe the behavior of traffic networks as self-similar processes with multifractal characteristics.

Several techniques have been developed for network traffic prediction using multifractal fundamentals. The Multifractal - ARlMA predictor is proposed for the analysis and prediction of VBR video traffic [10]. The mixed logical dynamical framework is used to model a multiserver system as a nonlinear system adapted to control the data flow of multiple servers [11]. In the pinnacle of 3G technology, mobile internet data traffic was modeled with the fractional autoregressive integrated moving average (FARIMA) exhibiting significant multifractal characteristics [12]. Finally, the work presented hereby seeks to generate traffic in the Wi-Fi band using the multifractal kernel of multiplicative cascades.

The remainder of this article is organized as follows. Section 2 details the current work related with spectrum prediction. Section 3 describes the mathematical foundation of the predictive model. In section 4, the results obtained for the traffic prediction of a W-Fi scenario are shown. Lastly, a set conclusions on the overall work are presented in section 5.

2. Related Works

Other developments can be considered relevant and are worthy of being mentioned here. Even though they do not use the previously discussed prediction techniques, they represent significant contributions in the field of spectrum prediction. In [13], routing and topology control problems are studied in mobile ad hoc networks (CR-MANETs) leading to a cognitive topology control scheme based on distributed prediction (PCTC) to provide greater routing capacities in CR-MANET. In [14], secondary users (SU) take advantage of online learning techniques for the regression of the received transmission power in different licensed frequency bands. Furthermore, the probability of the primary user (PU) state that can be busy or inactive is predicted based on the results of the power regression. The proposed strategy not only saves time and energy, but also improves the performance of unlicensed users. In [15], a new modeling method for spectrum measurement is proposed with various essential frequency bands through Daubechies waves. The method uses spectrum analysis and predicts based on regression. The strategy in [16] consists on combining spectrum prediction and monitoring techniques through the AND and OR fusion rules, for the detection of licensed users emerging in data transmission. The authors in [17] propose a new MAC called sense-and-predict (SaP), where each secondary transmitter (TX) decides whether to access or not the spectrum according to the predicted interference level in the receiver (RX). In [18], a new stochastic cognitive anti-jamming game model is used in multi-agent environments where each autonomous broadband cognitive radio seeks to predict and avoid transmissions from other radios and dynamic interference signals.

3. Materials and Methods

3.1 Data Collection

The research in [19] provided the nominal power values of the electric radio spectrum of Bogotá, Colombia. The information was acquired with a spectrum analyzer carrying out data traffic detection. The absence or presence of traffic was determined for the GSM, Wi-Fi and 1850–2000 MHz bands. The equipment used to register the spectral measurements included: a Discone antenna in the frequency range between 25 MHz and 6 GHz, a low noise amplifier (LNA) in the operating frequency range between 20 MHz and 8 GHz, and a power spectrum analyzer in the operating frequency range between 9 kHz and 7.1 GHz [20]. Measurements were carried out in six locations around the city. The main technical parameters of the captured data are a band resolution of 100 kHz, a span of 50 MHz and a time resolution of 333 ms [19].

This research focuses on the data of the Wi-Fi band. The information gathered comes from 461 frequency channels, with a time resolution corresponding to one-third of a second. In total, the Wi-Fi database has 85% training data (4,978,800) and 15% evaluation data (829,800). In 2015, the authors in [20] conducted a preliminary study to obtain an availability matrix describing the occupancy of primary users in the radio electric spectrum of Bogotá. A value of 1 in the matrix corresponds to an available time-frequency space while a 0 is a non-accessible space. The power values of the 461 channels are compared element-wise with a specific threshold. The tool proposed in [20] transforms the power data within the -40 to -147 dBm range into binary values according to the restriction set by a threshold.

Based on the availability matrix of the Wi-Fi band, it is proposed to create a time series that collects user download packages in time units and the availability of consecutive time instants within a channel. This reorganization of data has the purpose of building a time series revealing and thereby measuring channel fluctuations between occupied and available states as shown in Figure 1a.

For the generation of the time series, positive weights are assigned to the time instants in which the channel is free and negative weights are assigned to the occupied moments. A counting process of the positive and negative time units was performed so that the newly obtained time series contains consecutive intercalated available packets, followed by the packets occupied by users. Therefore, said series has positive values indicating free time units and negative values for occupancy-related units as shown in Figure 1b. The process is iterative for all channels included in the availability matrix.

3.2 Multifractal Traffic

The traditional tool for modeling and analysis of network traffic had been the classical Poisson traffic model, which was later adapted for queuing systems [21]. The measured traffic started revealing behaviors that were different from what was expected by the Poisson and Markov models. The data collected in Bellcore labs paved the way to study scale invariance for LAN traffic characterization [22]. Traditional time series models have proved to be insufficient to model traffic self-similarity so the analysis of such processes called for new techniques. Some models based on monofractal procedures were proposed to attempt to shape this traffic [23]. A recent analysis of the measured data revealed the existence of multifractal scaling behavior [8,24].

A process $X(t)$ is said to have local scaling properties with a local scaling exponent $\alpha(t)$ if the process behaves such that $X(\Delta t) \sim (\Delta t)\alpha(t)$ as $(\Delta t) \to 0$. In monofractal processes, the scaling exponent $\alpha(t) = H$ for all times while the scaling parameter $\alpha(t)$ is non-constant for multifractal scenarios. The local holder exponent is given by $\alpha(t)$ [25]. When the analysis is carried out in the scale domain with a wavelet transform, an estimation can be made of the coefficients containing the main information of signal $X(t)$ with the discrete wavelet transform (DWT) noted as $dx(j, k)$ (see (1) and (2)) [26].

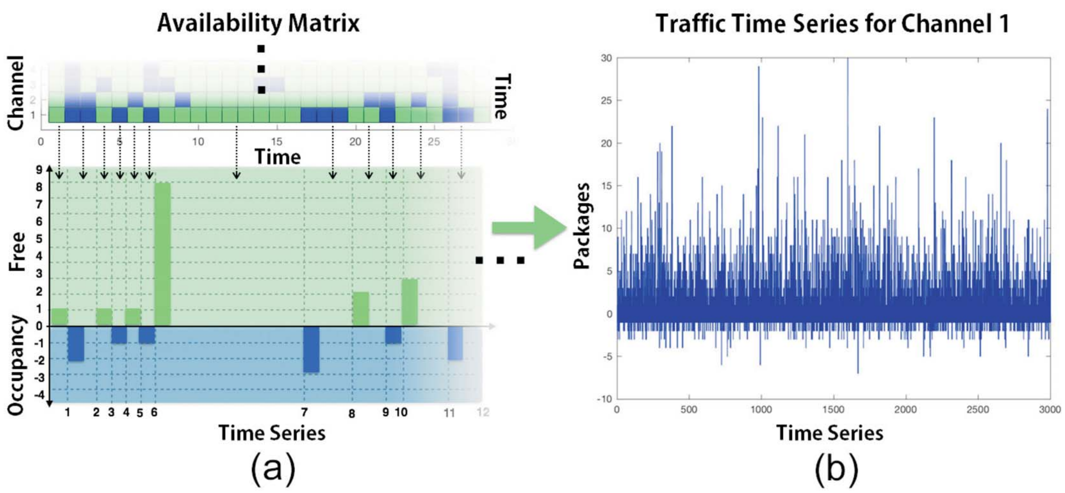

Figure 1. Building the time series based on the Wi-Fi availability matrix.

$$T_X(a,b) := \int_{-\infty}^{\infty} X(t)\psi\left(\frac{t-b}{a}\right)dt, \quad a,b \in \mathbb{R} \tag{1}$$

$$d_x(j,k) = T_X(2^j, 2^j k), \quad j,k \in \mathbb{R} \tag{2}$$

A fundamental characteristic of the continuous wavelet transform $Tx\,(a, b)$ is its redundancy, since neighboring coefficients share some common information regarding X. In fact, in order to reduce the redundancy from the inner product of the signal and the set of dilations (a) and shifts (b) of a mother wavelet Ψ (·), the DWT is introduced for all jth scales. The variance of $dx(j, k)$ can be estimated as μj, with the most relevant characteristics following the scaling behavior of the original signal (see (3) and (4)).

$$\mu_j = \frac{1}{n_j}\sum_{k=1}^{n_j} \left|d_x(j,k)\right|^2 \tag{3}$$

$$\mu_j \approx E[|d_x(j,k)|^2] \propto 2^{j(2H-1)} \tag{4}$$

The Hurst parameter H can be estimated by calculating the linear regression slope of yj against j. This representation is called the log-scale diagram (LD) of Equation (5).

$$y_j = \log_2 \mu_j = (2H-1)\,j + \log_2 C \tag{5}$$

Estimating H is useful to study second-order statistics (q = 2) of stochastic processes. Furthermore, the wavelet transform can be used for higher and lower statistic order in the real domain ($q \in R$). Consider the extension of μj to μjq and the estimator of μjq as shown in Equations (6) and (7).

$$\mu_j^{\,q} = \frac{1}{n_j}\sum_{k=1}^{n_j} \left|d_x(j,k)\right|^q \tag{6}$$

$$\mu_j^{\,q} \approx E[\left|d_x(j,k)\right|^q] = C_q 2^{j\left(\xi(q)-\frac{q}{2}\right)} \tag{7}$$

A monofractal process could be described as $H(q) = H\ \forall\ q \in \Re$, meaning that the Hurst parameter is the same for all statistics orders. When $H(q)$ decreases based on statistical orders the process is multifractal. The linear multiscale diagram (MD) plots the singularity exponent $H(q)$ of order q versus q, describing the behavior of H for different orders.

The multifractal spectrum (MS) plots $H(q)$ versus the singularity dimension $D(q)$. These two variables are a linear transformations of scales into statistical moments. Therefore, the function mapping the sampling scales with the respective statistical moments is non-linear. $D(q)$ can be estimated using the mass exponent τ (q) of order q shown in (8) and (9).

$$\tau(q) = q \cdot H(q) - 1 \tag{8}$$

$$D(q) \equiv \frac{\tau(q)}{q-1} = \frac{q \cdot H(q) - 1}{q-1} \tag{9}$$

The MS for a pure monofractal process is a point in space. In contrast, a multifractal time series is a concave curve pointing towards the x-axis. This form can be approximated to a second-order polynomial function whose width can be found by zero-crossing the function when $D(q) = 0$. This width is called the multifractal spectrum width (SW).

3.3 MFHSW

In 1999, Riedi et al. proposed in [27] a traffic generation model using a Conservative Binomial Cascade (CBC). The model was called the Multifractal Wavelet Model (MWM) and was based in the Haar wavelet transform, with the structure shown in (10).

$$W_{j,k} = A_{j,k}U_{j,k} \tag{10}$$

where $A_{j,k}$ is a random variable in the [-1, 1] interval. To make sure that $|Wj,k| \leq Uj,k$, the scale coefficients (j,k) have to be positive and zero-symmetric. Moreover, the multipliers $Aj,k = 2Bj,k$, are identically distributed random parameters within the [0,1] interval and symmetric to 0,5. The relation between the MWM and the multiplicative cascades takes place when the Haar transform serves as a multiplicative cascade coefficient by establishing the multiplicative coefficients as random variables, with an average of 0.5 in the [0,1] range. Therefore, the generation of positive data with multifractal characteristics is guaranteed. The MWM starts with U0,0 as the iteration value distributed for two intervals according to Bj,k and $Bj,k - 1$. The Bj,k value is a random number with a β distribution. Then, these values are distributed in the third scale into two with a different Bj,k for each couple. This process continues up to the Nth scale, leading to 2n intervals with U0,0 initial fractions. Therefore, the resulting CBC is given by (11).

$$W_{j,k} = \prod_{j=0}^{n} 2B_{j,k}U_{j,k} \tag{11}$$

where

$$PDF(B_{j,k}) = \begin{cases} \dfrac{1}{1-2^{j-1}} & \text{for } x \in [0,1] \\ 0 & \text{otherwise} \end{cases} \tag{12}$$

In 2012, Lopez et al. [26] proposed the multifractal-Hurst (MFH) algorithm to generate traces with positive data and long-range dependence. Since the MFW obeys to a power law, its fractal nature requires adjusting the Hurst parameter and its average. The wavelet coefficient multipliers are given by a β distribution with the relation in [30] for all scales of the CBC (see (13)).

$$B_{j,k} = k_h = \frac{2^{2H-1}-1}{2-2^{2H-1}} \therefore H \in [0.5,1] \tag{13}$$

When *kh* is adjusted with the expected value of *H*, it takes the same value of the parameter P defined in the multiplicative cascade method. A multifractal trace of length 2n is obtained with a given average and Hurst parameter. Finally, the MFH validates the value of *H* in the trace using the LD. If the estimation of H is not small enough to adjust to the confidence values, the trace is dismissed and a new one is generated. This process is repeated until H remains within the confidence values. Therefore, the CBC is built as indicated in Equation (14).

$$PDF(B_{j,k}) = \begin{cases} \dfrac{\Gamma(2k_h)}{\Gamma^2(k_h)} \cdot x^{k_h-1} \cdot (1-x)^{k_h-1} & \text{for } x \in (0,1) \\ 0 & \text{otherwise} \end{cases} \tag{14}$$

In 2016, Tuberquia et al. [28], proposed the multi-fractal-Hurst spectrum width (MHSW) algorithm to generate positive multifractal traffic with the mean, H and SW variables set by the user. This recent model distributes two kh throughout the scales of the CBC, instead of just one as seen in the MFH. In order to adjust the width of the multifractal spectrum, setting *kh* = *khw* in the last stage of the CBC would allow the modification of the spectrum. khw is computed by a series of experimental curves establishing its relation with the distribution of H in terms of the surrounding scales as shown in (15).

$$H_h + H_{hw} = \frac{0.5+1}{2} \tag{15}$$

In fact, *kh* is estimated with the Hurst parameter *Hh* of the final trace. The evaluation of *khw* is provided by *Hhw* (*js*, *Ws*), a linear function stating the relation between the scale where the cascade starts to change (*js*) and the desired multifractal SW (Ws). Thus, the CBC is defined as in (16).

$$W_{j,k} = \prod_{j=0}^{js} 2B_{1j,k}U_{j,k} \prod_{j=js}^{n} 2B_{2j,k}U_{j,k} \tag{16}$$

where

$$B_{2j,k} = k_{hw} = \frac{2^{2H_{hw}-1}-1}{2-2^{2H_{hw}-1}} \therefore H_{hw} \in [0.5,1]$$
$$H_{hw} = f(j_s, W_s) \tag{17}$$

*B*1*j*,*k* and *B*2*j*,*k* are random numbers with β distribution. The MFHW algorithm can be described as:

Algorithm 1: MFHW Synthesis

```
Input: U = Mean inter-arrival, n = length of trace,
       Hs = Desired Hurst, Ws = Desired MS Width
Output: Wjk = New_Trace
kh = (2^(2*Hh-1)-1)/(2-2^(2*Hh-1)); %Hh: Hurst parameter
Hhw = f(js, Ws);
khw = (2^(2*Hhw-1)-1)/(2-2^(2*Hhw-1)); %Hhw: Hurst
                   %parameter with width of the spectrum
Wjk=[U];
for i ← 1 to n
   if i < js then
      k = kh; %k adjusted with the expected value of H
   else
      k = khw; % k adjusted for width of the
      multifractal spectrum
   end
   for each Wjk[j]
      p = beta_rand(k);
      divide Wjk[j] in two (2*Wjk[j]*p,
      2*Wjk[j]*(1-p))
   end
end
ReturnWjk
```

3.4 LD, MD and MS for the Radio Electric Spectrum in Bogotá

In first place, the Hurst parameter is estimated for each channel of the radioelectric spectrum. The calculation of the variance estimator is based on the DWT. The slope is derived from the linear regression of yj against j. Channels with $0.5 < H < 1$ indicate a persistent trend in behavior and long-range dependence. Channels with $H > 1$ indicate an anti-persistent trend in behavior and series non-stationary. Out of the 461 channels, 25 were found with $H < 0.5$ (non-random discrete sequence), two with $H > 1$ and 434 remained in the [0.5, 1] range.

In second place, the MD is calculated for all channels in the spectrum. In the estimation process of $H(q)$, the channels showed some irregularities in terms of shape and organization thus related to the sampling procedure. In Figure 2a, the blue curve highlights an example of inadequate sampling. The proper selection of $H(q)$ is carried out by a hierarchical decision tree where the maximum value close to $q = 0$ is chosen for $H(q)$ which can then be compared to a sigmoidal-like curve. To properly estimate the width of the multifractal spectrum, as shown in Figure 2b, the blue curve represents the multifractal spectrum with inadequate sampling, where the calculation of the multifractal spectrum width is complex to perform.

After the sampling correction of the MD curve, the green curve can be obtained as shown in the Figure 2a. The curve descends when q goes from negative towards positive values. Similarly, the calculation of the MS width in Figure 2b shows that it is more precise for the green curve. Once the MDs have been corrected, the spectral widths are calculated in order to verify the multifractality of the time series derived from traffic in Bogotá.

The spectral widths have an average of 1.2072, a standard deviation of 0.3647, a minimum value of 0.7285 and a maximum value of 4.7910. Lastly, the estimation of H (q) and D (q) for all channels of the radio electric spectrum leads to an accurate traffic generation using the MFHW algorithm. The procedure is described in Algorithm 2.

Algorithm 2: MFHW for generation of CR traffic

Input: *Availability_Matrix*
Output: *New_Traffic*
for *ch* ← 1 to the last channel of availability matrix
    New_Time_Series(ch) ← *Signal_Adaptation (Availability_Matrix(ch))*;
    H_h*(ch)* ← *Hurst_Parameter_Estimation (New_Time_Series(ch))*;
    K_h*(ch)* ← *Beta_Coefficients(H1(ch))*;
    W_s*(ch)* ← *MS_Width_Estimation (New_Time_Series(ch))*;
    K_{hw}*(ch)* ← *Beta_Coefficients(W1(ch))*;
    while $|W_s(ch)-W| < 0.1$ **do**
        while $|H_h(ch)-H| < 0.05$ **do**
            trace ← *MFHW(K1,K2)*;
            H ← *Log_Scale_Diagram(trace)*;
            W ← *Multifractal_Spectrum_Diagram(trace)*;
        end
    end
    New_Traffic(ch) ← *trace*;
end
Return *New_Traffic*

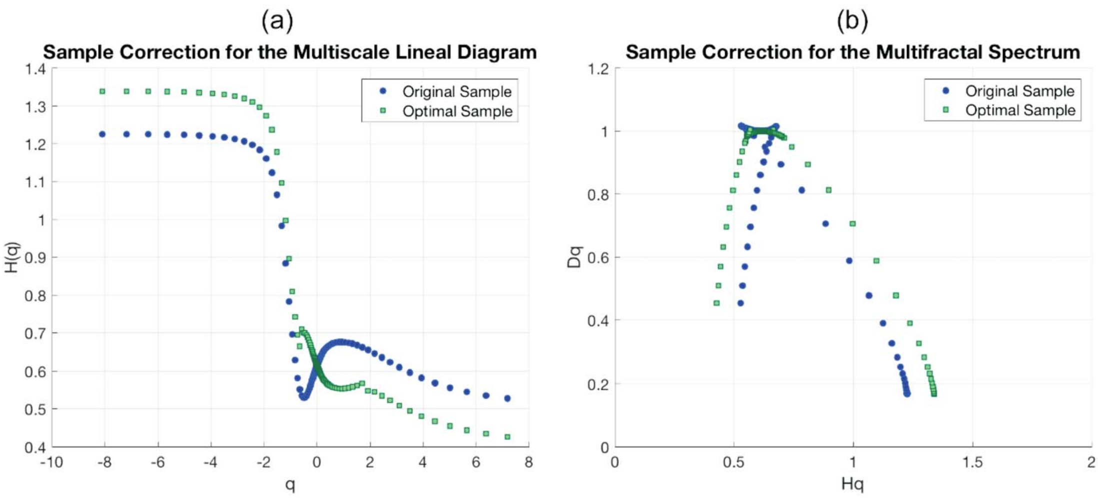

Figure 2. Before and after optimal sampling a) MD, b) MS.

4. Result Discussions

Regarding the values of H for each traffic series, the analysis presented in this research confirms that H ranges between 0.5 and 1. This indicates a self-similar behavior in the series and an asymptotic trend of the autocorrelation functions. It ensures that said series have a hyperbolic trajectory in the 'tails' of the distribution, offering a response far from exponential. The central limit theorem for self-similar processes reinforces the use of the autocovariance function on said processes within the [0.5, 1] interval, directly depending on the value of H [23].

In Figure 3, the blue markers correspond to the original estimations of H while the green markers correspond to the estimated values of H derived from traffic prediction. The black lines represent the errors between the expected and generated values. The overall error prediction for the Hurst parameter is 4.0547%.

Moreover, multifractality is related with the cases in which H is non-constant throughout the scale. This reveals a more stochastic nature in comparison to self-similar behavior or LRD. The results for the multifractal spectrum in traffic prediction are shown in Figure 4.

Figure 4 shows the spectral widths for the original time series in blue and the spectral MFHW estimates from traffic prediction in green. The black lines denote the error between the expected and generated values. The overall prediction error for the spectral width is 8.8583%.

100 consecutive channels and 100 time instants were compared between the original and predicted availability matrices. The resulting error is 33.67%. From left to right, Figure 5 shows the original channels, the predicted channels using the MFHW method and the errors.

5. Conclusions

This article discusses the study of non-constant responses for the Hurst parameter H throughout a constructive multifractal model in order to generate and characterize traffic flow in high-speed computer networks. The main purpose was to provide a prediction tool for multifractal traffic. Using the MFHW algorithm, essential characteristics were obtained that describe the analyzed traffic. The prediction values for the multifractal spectrum width and Hurst parameter were less than 0.1 and 0.01 respectively. Nevertheless, it is recommended to expand the MFHW algorithm thus increasing the accuracy of the newly obtained traffic and improve the results for the availability matrix in the radioelectric spectrum of the city of Bogotá.

Acknowledgements

The authors would like to thank Colciencias and Universidad Distrital Francisco José de Caldas for funding this research project.

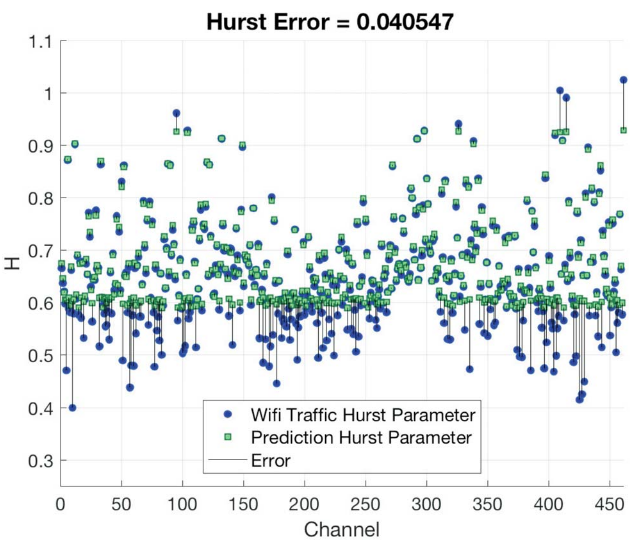

Figure 3. Hurst error for prediction of channels in the radioelectric spectrum of Bogotá.

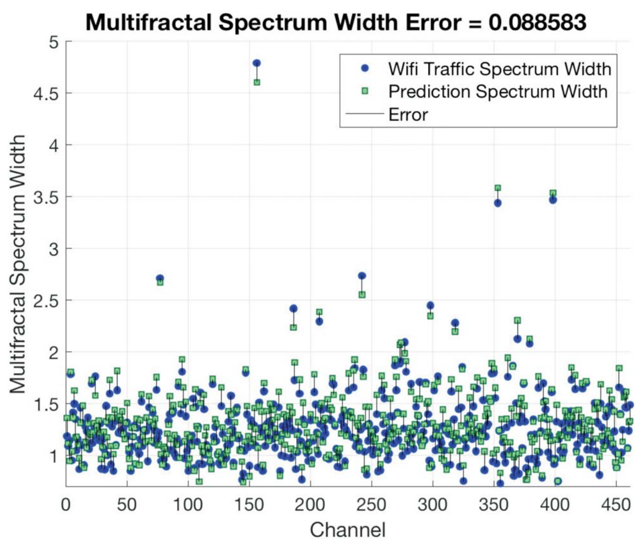

Figure 4. Multifractal SW error for channel prediction of the radio spectrum in Bogotá.

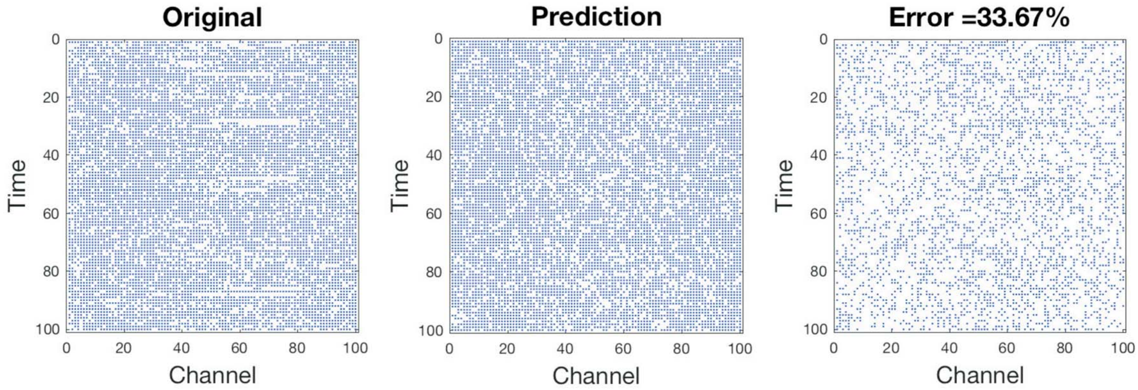

Figure 5. Availability matrix comparison between the original and predicted versions.

References

[1] Al-Tahmeesschi, A., M. López-Benítez, J. Lehtomäki, and K. Umebayashi (2017) Investigating the estimation of primary occupancy patterns under imperfect spectrum sensing, Proc. of 2017 IEEE Wireless Communications and Networking Conference Workshops, San Francisco, USA, 1–6. doi: 10.1109/WCNCW.2017.7919112

[2] Spectrum Policy Task Force (2002) Public comment on issues related to commission's spectrum, Federal Communications Commission, Report ET Docket No. 02-135, USA.

[3] Bernal, C., and C. Hernández (2019) *Modelo de Decisión Espectral Para Redes de Radio Cognitiva*, 1st Ed. UD, Bogotá, Colombia.

[4] Ding, G., J. Wang, Q. Wu, Y. D. Yao, F. Song, and T. A. Tsiftsis (2016) Cellular-base-station assisted device-to-device communications in TV white space, *IEEE Journal on Selected Areas in Communications* 34(1), 107–121. doi: 10.1109/JSAC.2015.2452532

[5] Frisch, U., and G. Parisi (1985) On the singularity structure of fully developed turbulence in turbulence and predictability in geophysical fluid dynamics and climate dynamics, Proc. of 1985 International School of Physic Enrico Fermi, North-Holland, 71–88.

[6] Leland, W. E., and D. V. Wilson (1991) High time-resolution measurement and analysis of LAN traffic: implications for LAN interconnection, Proc. of IEEE Conference on Computer Communications, Bal Harbour, USA, 1360–1366. doi: 10.1109/INFCOM.1991.147663

[7] Taqqu, M. S., V. Teverovsky, and W. Willinger (1997) Is network traffic self-similar or multifractal? *Fractals* 5, 63–73. doi: 10.1142/S0218348X97000073

[8] Riedi, R. H., and J. L. Vehel (1997) Multifractal properties of TCP traffic: a numerical study. *Institut National de Recherche en Informatique et en Automatique* 3129, 1–40.

[9] Ma, S., and C. Ji (1998) Modeling video traffic in the wavelet domain. In INFOCOM '98. Seventeenth Annual Joint Conference of the IEEE Computer and Communications Societies. Proceedings. IEEE. San Francisco, CA, USA. doi: 10.1109/INFCOM.1998.659655

[10] Shenghui, W., and Q. Zhengding (2006) Multifractal analysis and prediction of VBR video traffic, 2006 6th International Conference on ITS Telecommunications Proceedings, 0–3, Chengdu, China: IEEE. doi: 10.1109/ITST.2006.288848

[11] Hong, L., Y. Tie, and W. Lanlan (2010) Network traffic prediction based on multifractal MLD model, 2010 International Workshop on Chaos-Fractals Theories and Applications (IWCFTA), 466–470, Kunming, Yunnan, Chin. doi: 10.1109/IWCFTA.2010.109

[12] Yu, Y., M. Song, Y. Fu, and J. Song (2013) Traffic prediction in 3G mobile networks based on multifractal exploration, *Tsinghua Science and Technology* 18(4). doi: 10.1109/TST.2013.6574678

[13] Guan, Q., F. R. Yu, S. Jiang, and G. Wei (2010) Prediction-based topology control and routing in cognitive radio mobile ad hoc networks, *IEEE Transactions on Vehicular Technology* 59(9), 4443–4452. doi: 10.1109/TVT.2010.2069105

[14] Zhang, Z., K. Zhang, F. Gao, and S. Zhang (2015) Spectrum prediction and channel selection for sensing-based spectrum sharing scheme using online learning techniques, 2015 IEEE 26th Annual International Symposium on Personal, Indoor, and Mobile Radio Communications (PIMRC), 355–359, Hong Kong, China: IEEE.

[15] Chen, Y., and H. S. Oh (2016) Spectrum measurement modelling and prediction based on wavelets, *IET Communications* 10(16), 2192–2198. doi: 10.1109/PIMRC.2015.7343323

[16] Thakur, P., A. Kumar, S. Pandit, G. Singh, and S. N. Satashia (2016) Performance improvement of cognitive radio network using spectrum prediction and monitoring techniques for spectrum mobility, Proc. of 2016 Fourth International Conference on Parallel, Distributed and Grid Computing, Waknaghat, India, 5−10. doi: 10.1109/PDGC.2016.7913208

[17] Kim, J., S. W. Ko, H. Cha, and S. L. Kim (2017) Sense-and-predict: opportunistic MAC based on spatial interference correlation for cognitive radio networks, Proc. of 2017 IEEE International Symposium on Dynamic Spectrum Access Networks, Piscataway, USA, 1−10. doi: 10.1109/DySPAN.2017.7920787

[18] Aref, M. A., and S. K. Jayaweera (2017) A novel cognitive anti-jamming stochastic game, Proc. of 2017 Cognitive Communications for Aerospace Applications Workshop, Cleveland, USA, 1−4. doi: 10.1109/CCAAW.2017.8001605

[19] Pedraza, L., F. Forero, and I. Paez (2013) Metropolitan spectrum survey in Bogota Colombia, Proc. of IEEE International Conference on Advanced Information Networking and Applications Workshops, Barcelona, Spain, 548−553. doi: 10.1109/WAINA.2013.177

[20] Hernández, C., and D. Giral (2015) Spectrum mobility analytical tool for cognitive wireless networks, *International Journal of Applied Engineering Research* 10(21), 42265–42274.

[21] Kleinrock, L. (1975) *Queueing Systems: Vol. I: Theory.* 1st Ed. John Wiley & Sons, Inc, New York.

[22] Leland, W. E., M. S. Taqqu, W. Willinger, and D. V. Wilson (1994) On the self-similar nature of ethernet traffic, *IEEE/ACM Transactions on Networking* 2(1), 1–15. doi: 10.1109/90.282603

[23] Millán, G. (2009) *Análisis de Autosimilaridad de Tráfico Telemático Restringido al Nivel de Red*, M Sc. thesis, Pontificia Universidad Católica de Valparaíso, Chile.

[24] Tuberquia-David, L. M., H. López, and C. Hernández (2019) *A Multifractal Model for Cognitive Radio Networks*, 1st Ed. UD, Bogotá, Colombia.

[25] Murali, K. P., V. M. Gadre, and U. B. Desai (2003) *In Multifractal Based Network Traffic Modeling*, 1st Ed. Springer, Boston, USA. doi: 10.1007/978-1-4615-0499-3_1

[26] López Chávez, H. I. and M. Alzate (2012) Generation of LRD traffic traces with given sample statistics, Proc. of 2012 IEEE Workshop on Engineering Applications, Bogotá, Colombia, 1−6. doi: 10.1109/WEA.2012.6220077

[27] Riedi, R. H., M. S. Crouse, V. J. Ribeiro, and R. G. Baraniuk (1999) A multifractal wavelet model with application to network traffic, *IEEE Transactions on Information Theory* 45(3), 992–1018. doi: 10.1109/18.761337

[28] Tuberquia-David, M., F. Vela-Vargas, H. López-Chávez, and C. Hernández (2016) A multifractal wavelet model for the generation of long-range dependency traffic traces with adjustable parameters, *Expert Systems with Applications* 62, 373–384. doi: 10.1016/j.eswa.2016.05.010

Manuscript Received: Mar. 14, 2019
Accepted: Aug. 6, 2019